RSC Advances

PAPER

View Article Online
View Journal | View Issue

Cite this: *RSC Adv.*, 2020, **10**, 2526

Role of supramolecular policosanol oleogels in the protection of retinyl palmitate against photodegradation

Yixing Tian and Nuria C. Acevedo *

Exposure of retinyl palmitate (RP) to ultraviolet radiation can lead to its photo-degradation and loss of biological activity. Therefore, there is a demand to explore new approaches to protect RP in an easy, economical and efficient way. The objective of this study was to explore the role of policosanol oleogels (PCOs) in the protection of RP from photodegradation. UV-blocking action was tested by placing a layer of PCO as a barrier between a UVA (365 nm) source and 1% RP in soybean oil. Effects of structural characteristics of PCOs cooled at different rates on RP photostability were also studied. The ability of PCOs to prevent radical-mediated reactions was assessed by measuring oil oxidative stability over storage time at 40 °C. The remaining % RP was measured by HPLC during 4 days of UVA irradiation. PCO blocked energy absorption from UVA and further dampened the UVA mediated ionic photodissociation and free radical reactions due to matrix immobilization. After 4 days of UV exposure, photodegradation of RP was reduced by 64% when a PCO layer was used as a barrier. Peroxide values (PV) and *p*-anisidine values (*p*-A.V.) of soybean oil (SO) were significantly higher than those of PCOs over storage time. Cooling rate processing played a significant role in RP protection; the faster the cooling rate, the higher the RP photostability. This study demonstrated that the protective mechanism of RP in PCOs is a combined effect of physical UV-barrier action, molecular immobilization and inhibition of the free radical-mediated reaction.

Received 26th September 2019
Accepted 6th January 2020

DOI: 10.1039/c9ra07820g

rsc.li/rsc-advances

Introduction

Vitamin A is an essential nutrient for humans and plays an important role in visual functions, reproduction, cell growth and maintenance.[1] Retinyl Palmitate (RP), the ester form of Vitamin A, is widely used in many products, including foods, drugs and cosmetics, since retinyl esters are chemically and thermally more stable than retinol. Nevertheless, retinoids have limited chemical and photochemical stability, that is strongly affected by environmental factors, including solvent, temperature and oxygen availability.[2,3]

Several studies have been carried out on the chemical decomposition pathways of retinol and its esters, including thermal isomerization, dehydration and oxidation.[4–6] It has been reported that esterification induced retinol to be more labile to photolysis.[7] UV irradiation can photo-excite retinol and its esters[8] and mediate photoreactions, including isomerization, degradation, and oxidation.[9–13]

Based on the known mechanism of RP photoreaction, several strategies have been explored to improve photostability of RP. The entrapment or encapsulation of vitamin A has been used as an approach to improve chemical and photochemical stability in different systems, such as emulsions,[14] hydrogels,[15] solid lipid nanoparticles,[16,17] polymer encapsulation.[18,19] Addition of antioxidants has also been used to protect vitamin A from photooxidation.[14,15] The chemical stability of RP in emulsions was reported to be associated to the physical stability of emulsion and the presence of a coherent gel-like structure in the system.[20] Solid lipid nanoparticles were found to provide physical UV-blocking action to protect RP from photoreactions.[16] In a previous study on self-assembled supramolecular gels, Wang *et al.*[21] stated that RP molecules were isolated in the chambers of the three-dimensional network structure and RP photostability was increased by reducing the molecular collisions and the degradation process of RP. It was found that encapsulated systems protected RP from hydrolysis and oxidation overtime, and improved the RP photostability.[15] The aforementioned authors also stated that the presence of an antioxidant improved the photostability of RP, which suggested that oxygen was a photodegradation partner.

Oleogels are solid-like gel systems where the liquid phase is oil.[22] Some studies have been performed on the encapsulation and delivery of bioactive compounds in oleogels, such as monoglyceride oleogel,[23,24] sorbitan monostearate oleogel,[25] and 12-hydroxystearic acid oleogel.[25] Sullivan *et al.*[26] reported that ethylcellulose oleogels can improve the oxidative stability of oil and of a bioactive compound entrapped in the system. Policosanol

Department of Food Science and Human Nutrition, Iowa State University, 2543 Food Science Building, Ames, IA 50011, USA. E-mail: nacevedo@iastate.edu; ytian@iastate.edu

organogels are really attractive and thus, selected for our study, owing to their significant gelation ability and desirable rheological properties.[27] In a previous study on policosanol oleogels (PCOs),[28] it was found that concentrations of policosanol (PC) in liquid soybean oil within the 7–12% (w/w) formed a gel system with desirable solid-like behavior. In the mentioned work, it was demonstrated that PCO efficiently improved the photostability of RP entrapped in these PC-based oleogel system.[28] Nevertheless, the role played by PCO on RP protection has not been studied.

The overall goal of this study was to investigate the function of PCO systems on the protection of RP from degradation initiated by UV irradiation. Due to PCOs structural properties and their similarities with solid lipid nanoparticles and supramolecular hydrogels, we hypothesize that PCOs can act as a physical UV-barrier, provide immobilization of RP in the system and delay free radical-mediated reaction.

To test the stated hypothesis, this study was designed to evaluate RP protection from three aspects: the physical UV-blocking action, the effect of oleogel structure, and the delay or hindering of free radical-mediated reactions. Based on the results obtained in our previous study, 7% PCO (w/w) was chosen as matrix to study the mechanism of RP protection due to its higher efficiency to protect RP activity and low gelator concentration.[28] Furthermore, PCOs at two different concentrations (7% and 12%) prepared at different cooling rates were selected as systems to study the effect of oleogel structure. Remaining RP after UVA irradiation, microstructure of PCOs, location of RP in the system, matrix mobility, and oil binding capacity were analyzed to relate PCOs structure to RP protection. Peroxide values (PV) and *p*-anisidine values (*p*-A.V.) were measured to determine oil oxidative stability in PCOs over storage time and establish the matrix ability to prevent radical-mediated oxidation reactions. Soybean oil is a commonly used oil in the US and thus, was chosen as the liquid phase for our study.

Material and methods

Materials

Soybean oil (SO) was generously provided by ADM oils (Decatur, IL, USA). 98% Policosanol (PC) containing 60% octacosanol was purchased from PureBulk Inc. (Roseburg, OR, USA). RP (1 600 000–1 800 000 USP units per gram) and 2-propanol (HPLC grade) were purchased from Sigma-Aldrich (St. Louis, MO, USA). Hexane (HPLC grade), ethyl ether, isooctane, glacial acetic acid, potassium iodide, and sodium thiosulfate were from Fisher Chemical (Fair Lawn, NJ, USA). *p*-Anisidine (99%) was acquired from ACROS Organics (New Jersey, USA).

A UVA lamp Model ENF-280C (365 nm, 115 V, 60 Hz, 0.20 A) was used for UV treatment (Spectroline, NY, USA). The lamp provides 1.488×10^{-6} W cm^{-2} measured by UV safety meter model 6D (Solar Light, Glenside, PA, USA).

Oleogel preparation and UVA irradiation

Policosanol (7 and 12%, w/w) was added to soybean oil. The samples were heated at 85 °C and stirred at 250 rpm for 30 minutes. RP (1%, w/w) was added and slightly mixed after stirring. Samples were poured to completely fill Petri dishes of 35 mm diameter and 4 mm height, and cooled at the desired cooling rate according to the test to be performed. 7% PCOs were cooled at 2, 8, 25 °C min^{-1} and 12% PCOs were cooled at 8, 14, 25 °C min^{-1}. Different cooling rates were achieved by placing the samples at different storage temperatures and measuring the resulting cooling rate. For instance, cooling rates of 2, 8, 14 and 25 °C min^{-1} were obtained by placing the samples in a 4 °C refrigerator, −18 °C freezer, −80 °C freezer and container cooled with liquid nitrogen, respectively. Once cooled, samples were stored at 4 °C for one week before UVA treatment. Liquid SO with 1% RP (RP-SO) was prepared under the same conditions and used as control. For UVA irradiation, sample dishes were placed under the UVA lamp (365 nm) at 10 cm distance from the bottom of the dish and irradiated for 0, 0.5, 1, 2, 3, and 4 days.

Study of UV-blocking action

An UV irradiation study was conducted in order to test the physical UV-blocking action provided by the PCO network. The setup of the experiment is shown in Fig. 1. From left to right, 1% RP in 7% PCO (RP-PCO) was placed directly under the UVA (365 nm) lamp. An empty Petri dish and a layer of SO were placed on top of 1% RP in SO (RP-SO) dishes to account for the UV blockage of the Petri dish material and liquid oil. A standardized layer of 7% PCO (w/w) was placed on top of 1% RP in soybean oil (RP-SO) as a barrier under UVA irradiation. An additional control of SO on top of RP-PCO was used.

7% PCOs and SO with 1% (w/w) RP were prepared as explained in the previous section and cooled at a rate of 8 °C min^{-1}. Equal amounts of sample were poured in identical Petri dishes (35 mm diameter and 4 mm height) to ensure sample size consistency. Samples were irradiated for 0, 0.5, 1, 2, 3, and 4 days with an UVA lamp placed at 10 cm distance from the dishes. The % remaining all-*trans* RP was measured by high performance liquid chromatography (HPLC) after irradiation as explained in the following section.

RP determination by HPLC

After UVA irradiation, samples were analyzed by high performance liquid chromatography (HPLC). Samples were transferred to HPLC amber vials and diluted with hexane to a RP concentration range from 0.01 to 0.1 mg mL^{-1}. At least three replicates of each samples were analyzed.

A method developed by Scalzo *et al.*[29] with modifications was used to determine the residual concentration of *trans*-RP after UVA treatment by using normal phase HPLC. The HPLC instrument (Agilent 1100 Series LC/MSD Ion Trap; Santa Clara, CA, USA) was equipped with a diode array detector (DAD) G1315B (Agilent, Santa Clara, CA, USA). Analyses were carried out with a 50 mm × 4.6 mm SUPELCOSIL™ LC-Si (5 μm) column (Sigma-Aldrich, St. Louis, MO, USA). Mobile phase A hexane : isopropanol (99 : 1, v/v) and mobile phase B ethyl ether were used as mobile phase solvent. The amount of ethyl

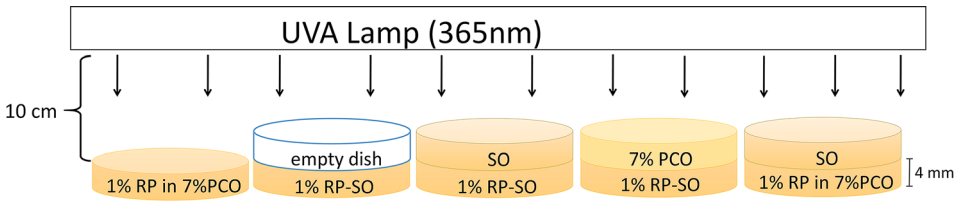

Fig. 1 Diagram showing the experimental setup of the UV-blocking action study.

ether was increased from 0 to 5% (v/v) over 5 min and then decreased to 0% during the following 2 min. The flow rate was 1 mL min^{-1} and the sample injection volume was 10 μL. The detector was set at 325 nm and the reference wavelength was 360 nm.

The HPLC chromatogram was integrated by Quant analysis for 6300 Series Ion Trap LC/MS version 1.8 (Agilent, Santa Clara, CA, USA). The remaining RP (%) was calculated by using the following equation:

$$\text{Remaining RP } (\% = \frac{\text{peak area of RP } (X \text{ d UV})}{\text{peak area of RP } (0 \text{ d UV})} \times 100\% \quad (1)$$

disc molds (22 mm diameter and 3.2 mm thickness). Samples were cooled at the specific cooling rates stated in previous section and stored at 4 °C for a week before analysis. Each oleogel disc was removed from the mold, placed on a round filter paper (Whatman #5, 110 mm diameter) and incubated at 20 °C. The weight of each filter paper was recorded after 0, 24, and 48 hours of storage time. A filter paper without sample on it was used as control in the experiments to account for the environment effect on the filter papers. Filter papers were large enough to absorb all the oil released from samples during the experiment without saturation. At least 10 replicates were prepared and means and standard deviations are reported. Oil loss (%) was calculated by using the following equation:

$$\%\text{Oil loss} = \frac{[\text{wt. paper}(x \text{ h}) - \text{wt. paper}(0 \text{ h})] - [\text{wt. blank}(x \text{ h}) - \text{wt. blank}(0 \text{ h})]}{\text{total mass of sample}} \times 100 \quad (2)$$

Microstructure

Differential interference contrast (DIC) microscopy was used to analyze the microstructure of the PCO samples. A small drop of hot liquid sample was placed between a preheated microscope slide and glass cover. The slides were heated and the cooled at a desired rate by using a PE120 cooling stage (Linkam Scientific Instruments, Tadworth, UK). Once prepared, the slides were stored at 4 °C for a week before observation. The images were acquired with a DIC microscope (Olympus BX53, Olympus Corporation, MA, USA) using the CellSens Dimension software (Olympus Corporation, MA, USA). Three replicates were prepared and 10 images of each slide were recorded. The images were analyzed by using software ImageJ (NIH, MD, USA) to report crystal particle area.

A fluorescence microscope was used to visualize the location of RP in SO and 7% PCOs since RP is fluorescent-active. The images were acquired with a Zeiss Axio Imager Z2 fluorescence microscope (Zeiss, Oberkochen, Germany) using the Zen Pro software (Zeiss, Oberkochen, Germany). Three replicates were prepared and 10 images of each slide were recorded.

Oil binding capacity

To test the oil binding capacity of PCO samples, discs were prepared by pouring the hot liquid oleogel mixture into PVC

Matrix molecular mobility

Matrix mobility of PCOs were measured by using a Bruker minispec mq-20 low-resolution spectrometer (Bruker Bio Spin Corporation, Billercia, MA, USA) operating at a resonance frequency of 20 MHz. Liquid PCO samples were poured into flat-bottom glass NMR tube (10 mm diameter, 180 mm length) up to a height of 1 cm, cooled at cooling rates ranging from 2 to 25 °C min^{-1} and afterwards stored at 4 °C for one week before testing. Each sample was prepared and analyzed in triplicate; means and standard deviations are reported.

The Carr–Purcell–Meiboom–Gill (CPMG) spin echo method was used to measure spin–spin relaxation time (T_2).[30,31] The instrument was set as a gain of 58 dB, 32 scans for signal averaging and 1.5 second (s) recycling delay. The delay interval was 0.04 millisecond (ms) and 4000 even echoes were sampled. Relaxation curves were fitted to a continuous distribution of exponentials using the CONTIN algorithm (Bruker software, Bruker BioSpin Corporation, Billerica, MA) between 0 and 1000 ms.

Analysis of oxidative stability

SO and 7% PCO samples with 1% RP were prepared to study the oxidation stability. Hot SO and 7% PCO samples were poured into flat-bottom glass vials (2 cm diameter, 8.5 cm length) up to

a height of 4 cm and cooled at 8 °C min^{-1}. After storage at 4 °C for one week, samples were incubated at 40 °C for 35 days. Peroxide values (PV) and *p*-anisidine values (*p*-A.V.) were measured at 0, 3, 5, 15, 25, and 35 days using AOCS official methods.[32] Each sample was analyzed in triplicate; means and standard deviations are reported.

Statistical analysis

Statistical analysis was carried out with Graph Pad Prism 5 (GraphPad Software, Inc., La Jolla, CA, USA). One-way analysis of variance (ANOVA) tests were conducted with Tukey's post-test to perform multiple comparisons. Significant differences were defined as p-value < 0.05.

Results and discussion

Study of UV-blocking action

A layer of 7% PCO was placed on the top of 1% RP-SO to assess if PCO can provide physical UV-blocking action to protect RP against light-mediated degradation, when compared with directly irradiated RP-PCO. An empty dish and a dish with liquid SO were also positioned between the light source and 1% RP-SO as controls to account for any additional UV-blockage caused by the dish material and the oil matrix. Chromatographs of the prepared samples are depicted in Fig. 2A–C. As reported in a previous study,[28] only the peak corresponding to all-*trans* RP, with 100% biological activity can be observed before irradiation.[33] The decrease of all-*trans* RP peak area and the presence of an additional peak corresponding to 9-*cis* RP (25% bioavailability),[33] upon UVA irradiation, are associated to RP degradation or isomerization.[28] As expected, it can be observed in Fig. 2A that the chromatograms of 1% RP SO with a SO top layer show a continue decrease in the all-*trans* RP peak with irradiation time. Furthermore, the additional peak corresponding to 9-*cis* RP can be observed particularly after 1–2 days irradiation of this sample indicating UVA mediated RP degradation and isomerization. The inset in Fig. 2A shows the enlarged region of the chromatogram where the 9-*cis* RP can be clearly observed. In this study, the reduction in the peak area over irradiation time is substantial for both controls (empty dish-data and SO top layer, Fig. 2D), which suggest a non-significant protection exerted by the dish material and the SO matrix. As can be observed in Figure 2D, 76% and 87% of RP was degraded when an empty dish or a layer of liquid SO was placed in the UV path during irradiation. Chromatograms obtained for the RP-SO sample with an PCO filled dish on top are depicted in Fig. 2B. The remaining all-*trans* RP in the RP-SO sample with a PCO top layer was significantly (p < 0.05) higher than the control samples upon all irradiation times; additionally, no 9-*cis* RP peak was observed. Similar chromatograms showing photodegradation hindrance of all-*trans* RP entrapped in 7% PCO samples (without top layer) are shown in Fig. 2C. The % RP remaining values in samples after UVA irradiation are

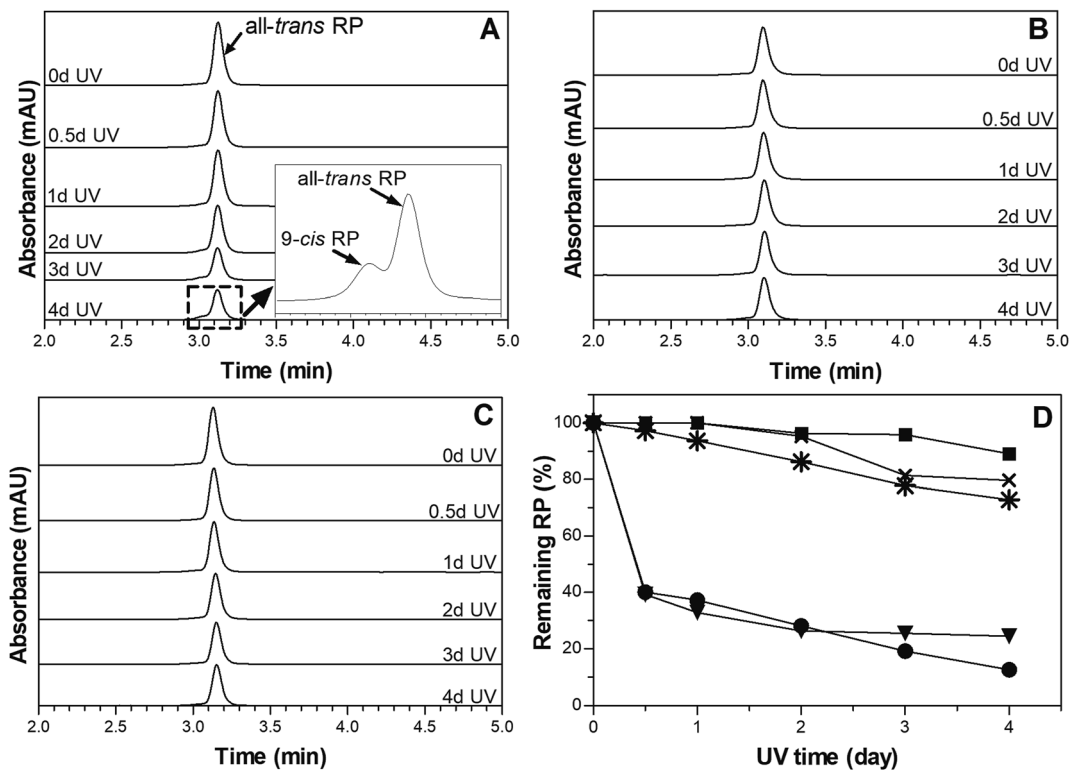

Fig. 2 HPLC chromatographs of (A) RP-SO with SO layer on top, (B) RP-SO with a 7% PCO (w/w) top layer and (C) RP-PCO; after different times (0, 0.5, 1, 2, 3, 4 days) of UVA radiation. (D) Remaining RP (%) values for all samples: (■) 1% RP-SO with 7% PCO top layer, (✖) 1% RP-PCO with SO top layer, (✱) 1% RP-PCO, (▼) 1% RP-SO with SO top layer, (●) 1% RP-SO with top empty dish.

shown in Fig. 2D. It can be observed that 7% PCO top layer can efficiently protect 1% RP-SO from photodegradation, which suggests that PCOs can block the energy absorption from UVA irradiation. Over 89% RP remained after 4 days of UVA irradiation; compared to the controls where approximately 25% and 3% RP remained with SO and an empty dish as top layer, respectively. Therefore, after 4 days of UV exposure, the PCO layer was capable to reduce RP degradation by 64%. As expected, liquid SO cannot prevent or delay RP photodegradation as no significant differences ($p < 0.05$) were observed between % remaining RP in PCO with and without a top layer of SO. Interestingly, the % remaining RP in the RP-SO with PCO top layer was 16% higher than that found in RP-PCO samples without top layer. This difference is probably because RP was homogenously distributed within the 7% PCO matrix and thus, some molecules dispersed close to the sample surface were more accessible to UV exposure.

Overall, as previously stated the findings of this study indicate that PCO matrices can block the energy absorption from UVA irradiation and protect RP from degradation. This effect is probably associated to the crystalline network present in PCO matrices. Crystal particle area size in 7% PCO were reported to be 148.3 $\pm$ 2.7 μm^2,[28] which can significantly block the UVA (365 nm) used in this experiment. Thus, 7% PCO provides an effective UVA obstruction to improve the photostability of RP. These results are in line with previous studies on RP stability where UV light was found to be physically blocked by the matrix. For instance, in a previous work, it was reported that solid lipid nanoparticles improved RP photostability over time through physical UV-blocking action.[16]

Microstructure

Microstructural properties of 7% and 12% PCOs prepared at different cooling rates were studied to establish the relationship between RP protection and crystalline network characteristics. Typical microscopy images of PCOs are shown in Fig. 3A–F. Large, needle-like crystals (Fig. 3A–C) generally characterize the microstructure of 7% PCO networks. At this relatively low PC concentration, thee large crystals were distributed far from another in the matrix without much interaction. As expected, with the increase in cooling rate during sample preparation (from 2 to 25 °C min^{-1}), the crystal particle area decreased from 166.4 $\pm$ 14.6 μm^2 (2 °C min^{-1} cooling rate) to 60.9 $\pm$ 5.2 μm^2 (25 °C min^{-1} cooling rate). Faster cooling rate associates with a higher time-dependent undercooling or supersaturation, which leads to faster rate of nucleation resulting in a higher population of small crystals.[34] Similar results were found in sunflower wax oleogels where rapid cooling decreased the crystal length and network pore area fraction.[35] The same trend was found in 12% PCOs prepared at different cooling rates with crystal areas decreasing from 55.0 $\pm$ 3.5 μm^2 at 8 °C min^{-1} to 26.9 $\pm$ 0.6 μm^2 at 25 °C min^{-1} (Fig. 3D–F). As expected, a higher PC concentration in the matrix promoted the growth and expansion of the crystalline structure due to the higher supersaturation. As a consequence, a dense network constituted by smaller crystallites and big crystalline aggregates was formed in

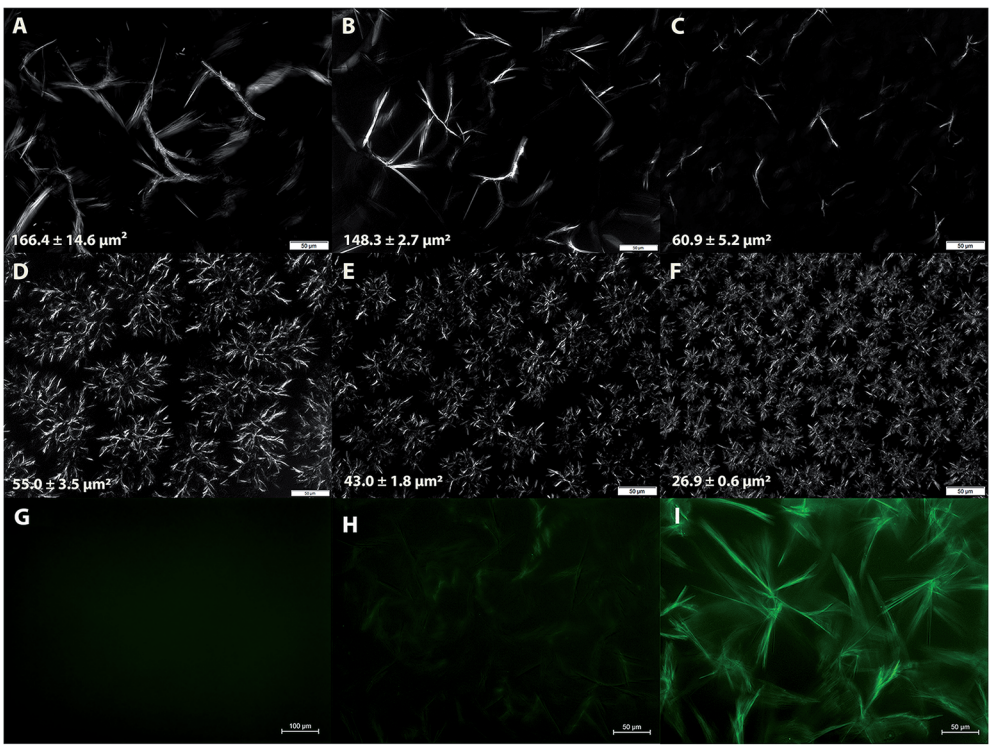

Fig. 3 Micrographs obtained by DIC microscopy of 7% and 12% PCOs (w/w) prepared at different cooling rates: (A) 7% PCO, 2°C min^{-1} (B) 7% PCO, 8°C min^{-1} (C) 7% PCO, 25°C min^{-1} (D) 12% PCO, 8°C min^{-1} (E) 12% PCO, 14°C min^{-1} (F) 12% PCO, 25°C min^{-1}. Fluorescence micrographs of (G) 1% RP in SO (H) 7% PCO (w/w) (I) 7% PCO with 1% RP.

12% PCOs. The obtained results confirmed that preparation cooling rate has a significant impact on the network microstructure formed in PCOs.

Representative fluorescence microscopy of SO and 7% PCOs with and without RP are shown in Fig. 3G–I. As expected, RP-SO did not show luminescence which indicates RP is homogeneously dispersed in liquid SO (Fig. 3G). Compared with 7% PCO (Fig. 3H), RP-PCO (Fig. 3I) shows a significantly enhanced luminescence, predominantly in the boundaries of the crystalline portions of the network. These results suggest that the crystalline structure can potentially immobilize RP in the matrix, which would be correlated to the improvement of RP photostability by reducing molecular collisions.[20] Similar results were reported by Wang *et al.*[21] that self-assembled supramolecular gels isolated RP in the "chambers" of three-dimensional networks, which protected RP from photodegradation. Similarly, it was found that ethylcellulose oleogels protected beta-carotene, which was located in the connected pockets within polymer network, through reducing the diffusion of beta-carotene.[26] It is noteworthy to mention that polymeric organogelators were used in the aforementioned studies and the PCs used in this study are low molecular weight oleogelators, while PCOs are crystal particle based oleogels. Nevertheless, despite their structural differences it seems that the crystalline network is able to isolate and immobilize RP, which probably leads to a reduction of molecular collisions and thus, inhibition of RP degradation.

Oil binding capacity

Oil binding capacity of PCO samples prepared at different cooling rates was analyzed through determination of oil loss values (% OL). The purpose was to study the PCO physical stability during short time storage at 20 °C and evaluate its relationship, if any, to RP photostability. % OL values obtained from all the PCO samples as a function of time are shown in Fig. 4. As expected, 7% PCO prepared at low cooling rate showed the highest % OL due to the large crystals created that are not connected to each other and thus, a weak network is formed (Fig. 4A). This frail network was not able to entrap liquid oil effectively, which led to OL values of 16.9 ± 1.4% and 24.2 ± 1.8% after 24 and 48 hours of storage, respectively. These results are in line with those of previous authors.[36] The mentioned authors reported that the presence of larger crystals formed as a result of fast cooling rates during crystallization led to a greater oil loss. Surprisingly, there was no significant difference ($p > 0.05$) found in 7% PCOs prepared at 8 and 25 °C min^{-1}. As shown in the microscopy images (Fig. 3A–C), smaller crystals were formed in 7% PCO prepared at 25 °C min^{-1} (60.9 ± 5.2 μm^2) than that prepared at 8 °C min^{-1} (148.3 ± 2.7 μm^2). However, the difference in crystal sizes did not significantly influence the oil binding capacity during short time storage. Both samples showed significantly ($p < 0.05$) lower OL values than the sample prepared at 2 °C min^{-1}. With low PC concentration (7%) in the system, when cooling rate reaches certain level (8 °C min^{-1}), the increase of cooling rate won't affect the OL in short time storage.

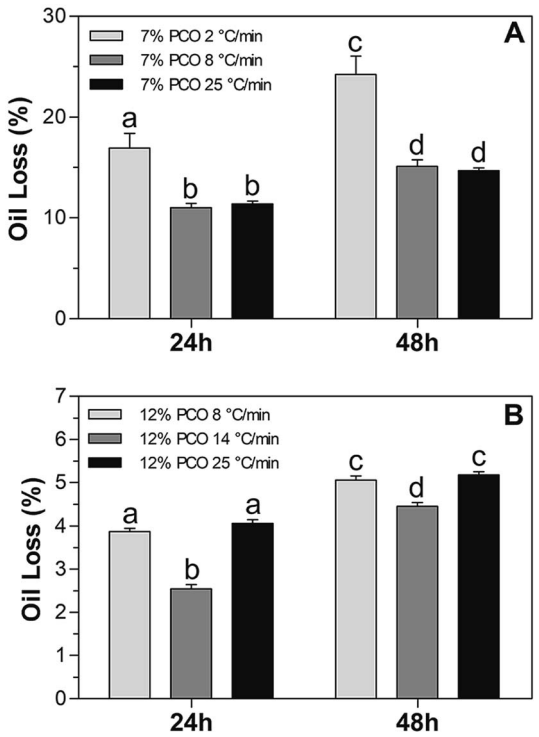

Fig. 4 Oil loss values (% OL) for (A) 7% and (B) 12% PCOs (w/w) prepared at different cooling rates. Different letters assigned to each bar represent statistically significant differences between the values across all samples ($p < 0.05$).

With higher PC concentration in the matrix, 12% PCOs showed significantly lower % OL values than 7% PCOs (Fig. 4B), which is associated with the smaller crystal particle area (Fig. 3D–F) and a more developed and stronger network formed in 12% PCOs. When sample's cooling rate was raised from 8 to 14 °C min^{-1}, the % OL values of 12% PCOs significantly decreased due to the decrease of crystal particle area in matrix as observed by microscopy. However, a further increase in cooling rate to 25 °C min^{-1} led to an increase in % OL values of 12% PCOs. As stated in our previous study,[28] 12% PCOs takes longer time to create a stable crystal network. At high cooling rate (25 °C min^{-1}), 12% PC in oil is not able to create a stable network and entrap liquid oil efficiently at short times after its formation. Therefore, the oleogel matrix released part of the oil not entrapped in the network during the initial stages of the oil loss test.

Effect of cooling rate on RP photostability

The % RP remaining after irradiation of 7% and 12% PCOs prepared at different cooling rates are shown in Fig. 5. For 1% RP in 7% PCOs, no significant differences ($p > 0.05$) were observed in % RP remaining between the different cooling rates used to prepare the samples (Fig. 5A). Despite a different microstructure (Fig. 3A–C) resulted from cooling at different rates, perhaps, the observed crystal size differences are not critically determining photoprotection in this type of network where large crystals sizes are present. Nevertheless, a trend where less % RP remaining is observed at PCO cooled slowly

when compared to PCO cooled at fast rates. These results may be partially related to the ability of the network to retain liquid oil and properly immobilize RP. As mentioned before, 7% PCO cooled at 2 °C min^{-1} showed a reduced oil binding capacity (high % OL, Fig. 4A) which agrees with the tendency to observe the lowest % RP remaining particularly after 24 and 48 h irradiation. Overall, all the 7% PCO samples efficiently protected RP from photodegradation regardless of the rate used to cool the samples; more than 70% RP remained after irradiation. Similarly, to 7% PCO, a trend characterized by an increase in the RP protection at fast cooling rates was observed in 12% PCOs. The small crystal particle areas and intricate network formed in 12% PCOs cooled fast from the melt can perhaps block energy absorption more efficiently than those developed at 7% PC levels, and provide better immobilization of RP molecules.

Matrix molecular mobility

Matrix molecular mobility was studied to assess contribution of matrix and RP molecular immobilization to the photoprotection of RP in PCOs. Measurement of the spin–spin relaxation times (T_2) gives information on the relative mobility of the matrix's molecular species. Short T_2 values suggest important interactions between adjacent molecules; therefore indicating a significant physical restriction within the matrix. On the other hand, long T_2 relation times suggest the predominance of more mobile species in the system. The respective spin–spin relaxation times (T_2) spectra of SO and PCOs prepared at different cooling rates are shown in Fig. 6. As expected, it was found that SO had a significantly ($p < 0.05$) higher T_2 value than PCOs regardless of the PC ratio and preparation cooling rate used in their formulation, which indicates PCOs immobilized matrix molecules in the network. It is possible to observe in Fig. 6B and C a trend where T_2 values of PCOs prepared at fast cooling rates show a shift to lower T_2 values when compared to those of PCOs cooled slowly. Furthermore, an incipient more mobile (larger T_2) second population appears at low cooling rates, in particular at 7% PCO. These results suggest that PCOs prepared at fast cooling rates seem to provide a more restricted matrix and thus, more RP immobilization; which can be directly connected to a more effective protection of RP. Surprisingly, these results are in line

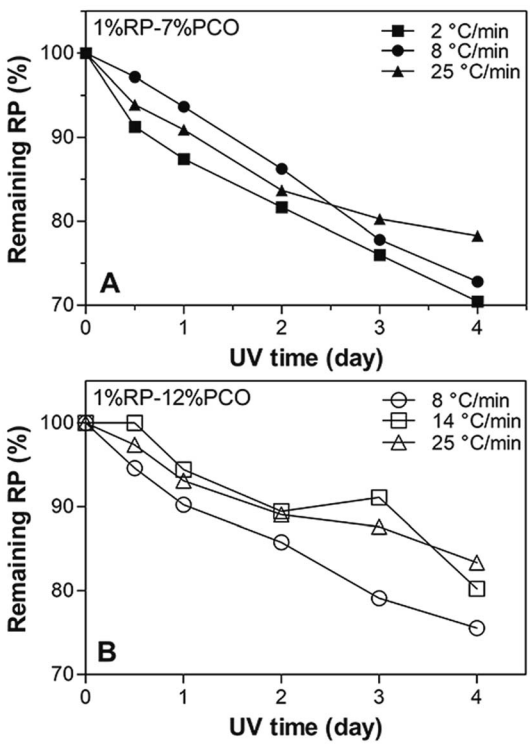

Fig. 5 Remaining RP (%) values in (A) 7% and (B) 12% PCOs (w/w) prepared at different cooling rates after different times (0, 0.5, 1, 2, 3, 4 days) of UVA radiation.

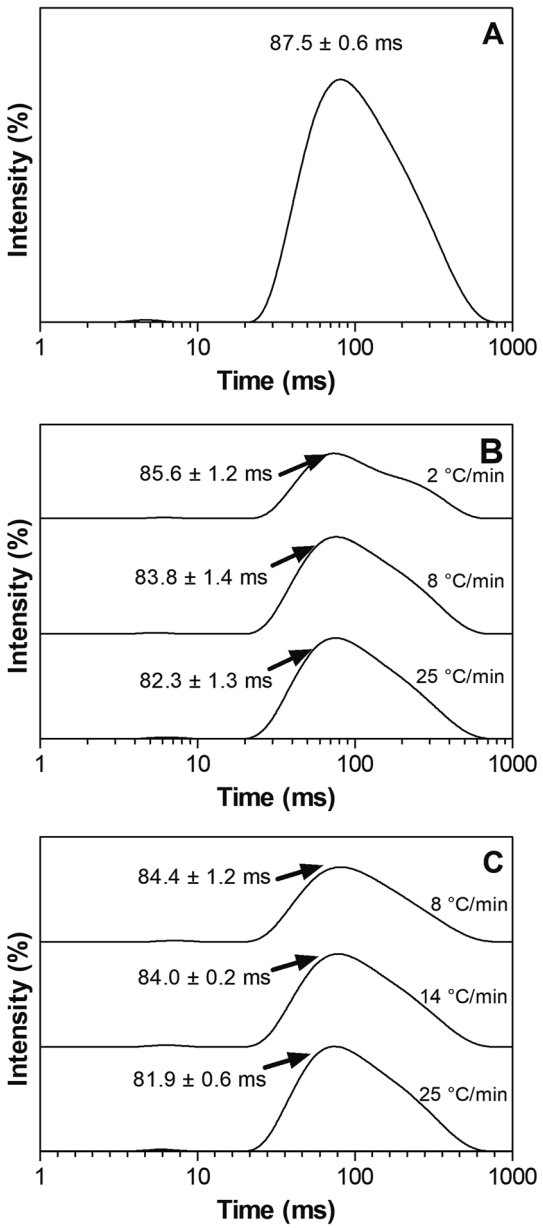

Fig. 6 NMR T_2 relaxation spectra of SO and PCO samples prepared at different cooling rates: (A) SO (B) 7% PCO (C) 12% PCO.

to the trends observed in Fig. 4 and 5 where a higher OL% and lower % RP remaining can be observed in PCO cooled slowly from the melt. At higher cooling rate, a high population of small crystals were formed in the matrix (Fig. 3), which resulted in enhanced molecular immobilization, oil binding capacity and RP protection. These findings agree with previous works where it was reported a much more restricted environment in the gelled state when compared to liquid oil.[37,38] These results agree with the previous findings obtained by fluorescence microscopy (Fig. 3G–I) showing that the PCO crystalline network was able to immobilize RP in the system and further reduced RP degradation by probably reducing molecular collision. Previous authors reported similar conclusions; for instance, Semenzato *et al.*[20] indicated that the chemical stability of RP depends on the physical stability and the presence of a coherent gel-like structure in an emulsion system.

Analysis of oxidative stability

Free radical-mediated reactions have been shown to be involved in the UVA mediated degradation of RP. Crank and Pardijanto[9] found that singlet oxygen initiated the photooxidation of RP and produced anhydroretinol and fragments derived from cleavage of the side-chain double bonds. It was found that vitamin A concentration decreased twice as fast in highly peroxidized soybean oil (PV > 10 mequiv. O_2 per kg) when exposed to fluorescent light, compared to vitamin A in a mildly oxidized oil (PV < 2 mequiv. O_2 per kg).[39] These authors pointed out that the oxidative status of the oil used for RP fortification has an impact on the stability of RP. PV is a common parameter used to characterize the oxidative state of oil, particularly the concentration of hydroperoxide; *i.e.* the primary oxidation products. *p*-A.V. indicates the amount of secondary oxidation products.[40] High PV and *p*-A.V. indicate the sample has undergone oxidation.

In order to investigate the oxidative stability of oil in PCOs and whether PCOs can potentially delay free radical-mediated reaction and therefore contributing to RP stability, PV and *p*-A.V. were measured over storage time at 40 °C (Fig. 7). It was found that SO samples have higher PV and *p*-A.V. than 7% PCOs over storage time and the differences became statistically significant ($p < 0.05$) upon 15 and 25 days of storage for PV and *p*-A.V., respectively. After 35 days storage time, the PV of 7% PCO was less than half (16.8 ± 0.8 mequiv. O_2 per kg) the PV found in liquid SO (34.3 ± 6.5 mequiv. O_2 per kg). PCOs improved the oxidative stability by entrapping the liquid oil in PCO network, reducing molecular collisions and hindering the advancement of free radical facilitated reactions. The high oxidative stability in PCOs is beneficial and contributes to improve the photostability of RP in the system which agrees with the reports by Pignitter, *et al.*, (2014).[39] Compared with liquid soybean oil, PCOs can prevent the free radical-mediated photooxidation of RP. These results suggest that PCOs can improve oil oxidative stability and potentially hinder effectively the progress of radical-mediated oxidative reactions.

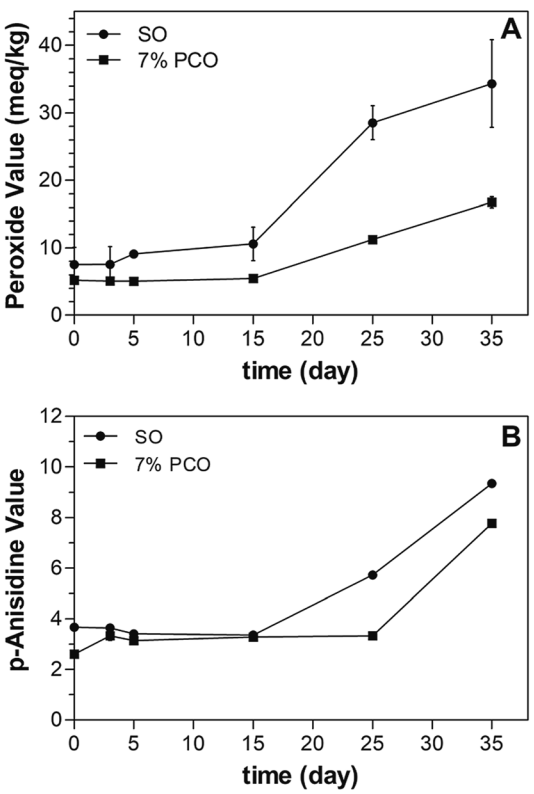

Fig. 7 Peroxide values (PV) and *p*-anisidine values (*p*-A.V.) of SO and 7% PCO incubated at 40 °C over time.

Conclusions

This work focused on the study of the role played by PCOs in the protection of RP upon light exposure. From the UVA blockage study, it can be concluded that PCOs could efficiently block UVA energy absorption and further protect RP from UVA mediated photodegradation. Cooling rate has a significant impact on the network structure formed in PCOs. 7% and 12% (w/w) PCOs prepared at higher cooling rates had smaller crystal particle area sizes and provided better RP protection due primarily to an enhanced molecular immobilization that can be detected by relaxation NMR studies. Fluorescence microscopy and low-resolution NMR results suggested that PCOs efficiently immobilized RP in the network and significantly reduced molecular collision. PV and *p*-A.V. of SO and 7% PCOs showed that PCOs are more stable to oxidation than liquid oil and thus, could effectively hinder the progress of radical-mediated oxidative reactions. Overall, the PCOs exert protection of RP to light degradation through a combination of a physical UVA blocking action, the immobilization of RP in the system and the inhibition or delay of oxidative free radical-mediated reactions.

Conflicts of interest

The authors declare no conflict of interest.

Acknowledgements

The authors acknowledge Dr Ann Perera, Dr Lucas Showman, and Dr Kirthi Narayanaswamy, from W. M. Keck Metabolomics

Research Laboratory for assisting with the HPLC method for retinyl palmitate analysis. This paper is a product of the Iowa Agriculture and Home Economics Experiment Station, Ames, Iowa. Project No. IOW03902 sponsored by Hatch Act and State of Iowa funds.

References

1 E. S. Tee and C. Lee, Carotenoids and retinoids in human nutrition, *Crit. Rev. Food Sci. Nutr.*, 1992, **31**(1–2), 103–163.
2 E. Deritter, Vitamins in pharmaceutical formulations, *J. Pharm. Sci.*, 1982, **71**(10), 1073–1096.
3 H.-G. Ji and B. S. Seo, Retinyl palmitate at 5% in a cream: its stability, efficacy and effect, *Cosmet. Toiletries*, 1999, **114**(3), 61–68.
4 J. K. McBee, V. Kuksa, R. Alvarez, A. R. de Lera, O. Prezhdo, F. Haeseleer, I. Sokal and K. Palczewski, Isomerization of all-*trans*-retinol to *cis*-retinols in bovine retinal pigment epithelial cells: dependence on the specificity of retinoid-binding proteins, *Biochem*, 2000, **39**(37), 11370.
5 M. Różanowska, A. Cantrell, R. Edge, E. J. Land, T. Sarna and T. G. Truscott, Pulse radiolysis study of the interaction of retinoids with peroxyl radicals, *Free Radic. Biol. Med.*, 2005, **39**(10), 1399–1405.
6 W. H. Tolleson, S.-H. Cherng, Q. Xia, M. Boudreau, J. J. Yin, W. G. Wamer, P. C. Howard, H. Yu and P. P. Fu, Photodecomposition and phototoxicity of natural retinoids, *Int. J. Environ. Res. Public Health*, 2005, **2**(1), 147–155.
7 H. Ihara, N. Hashizume, N. Hirase and R. SUZUE, Esterification makes retinol more labile to photolysis, *J. Nutr. Sci. Vitaminol.*, 1999, **45**(3), 353–358.
8 P. P. Fu, Q. Xia, J. J. Yin, S. H. Cherng, J. Yan, N. Mei, T. Chen, M. D. Boudreau, P. C. Howard and W. G. Wamer, Photodecomposition of vitamin A and photobiological implications for the skin, *Photochem. Photobiol.*, 2007, **83**(2), 409–424.
9 G. Crank and M. S. Pardijanto, Photo-oxidations and photosensitized oxidations of vitamin A and its palmitate ester, *J. Photochem. Photobiol., A*, 1995, **85**(1–2), 93–100.
10 M. Mousseron-Canet, Photochemical transformation of vitamin A, *Methods Enzymol.*, 1971, **18**, 591–615.
11 M. Mousseron-Canet, J. Mani, C. Favie and D. Lerner, On the photochemical isomerization of vitamin A, *C. R. Chim.*, 1966, **262**, 153–155.
12 K. Tsujimoto, H. Hozoji, M. Ohashi, M. Watanabe and H. Hattori, Wavelength-dependent peroxide formation upon irradiation of all-*trans* retinal in an aerated solution, *Chem. Lett.*, 1984, **13**(10), 1673–1676.
13 Q. Xia, J. J. Yin, W. G. Wamer, S.-H. Cherng, M. D. Boudreau, P. C. Howard, H. Yu and P. P. Fu, Photoirradiation of retinyl palmitate in ethanol with ultraviolet light-formation of photodecomposition products, reactive oxygen species, and lipid peroxides, *Int. J. Environ. Res. Public Health*, 2006, **3**(2), 185–190.
14 M. Carlotti, V. Rossatto and M. Gallarate, Vitamin A and vitamin A palmitate stability over time and under UVA and UVB radiation, *Int. J. Pharm.*, 2002, **240**(1), 85–94.
15 M. Carlotti, V. Rossatto, M. Gallarate, M. Trotta and F. Debernardi, Vitamin A palmitate photostability and stability over time, *Int. J. Cosmet. Sci.*, 2004, **26**(5), 270.
16 M. Carlotti, S. Sapino, M. Trotta, L. Battaglia, D. Vione and E. Pelizzetti, Photostability and stability over time of retinyl palmitate in an O/W emulsion and in SLN introduced in the emulsion, *J. Dispersion Sci. Technol.*, 2005, **26**(2), 125–138.
17 V. Jenning and S. H. Gohla, Encapsulation of retinoids in solid lipid nanoparticles (SLN), *J. Microencapsulation*, 2001, **18**(2), 149–158.
18 C. Duclairoir, J. M. Irache, E. Nakache, A. M. Orecchioni, C. Chabenat and Y. Popineau, Gliadin nanoparticles: formation, all-*trans*-retinoic acid entrapment and release, size optimization, *Polym. Int.*, 1999, **48**(4), 327–333.
19 Y. Çirpanli, N. ünlü, S. Çaliş and A. Hincal, Formulation and *in vitro* characterization of retinoic acid loaded poly (lactic-*co*-glycolic acid) microspheres, *J. Microencapsulation*, 2005, **22**, 877–889.
20 A. Semenzato, A. Bau, C. Dall'Aglio, M. Nicolini, A. Bettero and I. Calliari, Stability of vitamin A palmitate in cosmetic emulsions: influence of physical parameters, *Int. J. Cosmet. Sci.*, 1994, **16**(4), 139–147.
21 H. Wang, F. Fang, X. Li, C. Fu and Y. Yang, Improved photostability of Vitamin A palmitate originating from self-assembled supramolecular gels, *Chin. Sci. Bull.*, 2012, **57**(33), 4257–4263.
22 A. G. Marangoni and N. Garti, *Edible oleogels: structure and health implications*, Elsevier, 2011.
23 H. Yu, K. Shi, D. Liu and Q. Huang, Development of a food-grade organogel with high bioaccessibility and loading of curcuminoids, *Food Chem.*, 2012, **131**(1), 48–54.
24 S. Murdan, T. Andrýsek and D. Son, Novel gels and their dispersions—oral drug delivery systems for ciclosporin, *Int. J. Pharm.*, 2005, **300**(1), 113–124.
25 K. Iwanaga, T. Sumizawa, M. Miyazaki and M. Kakemi, Characterization of organogel as a novel oral controlled release formulation for lipophilic compounds, *Int. J. Pharm.*, 2010, **388**(1), 123–128.
26 C. M. Sullivan, M. Davidovich-Pinhas, A. J. Wright, S. Barbut and A. G. Marangoni, Ethylcellulose oleogels for lipophilic bioactive delivery–effect of oleogelation on *in vitro* bioaccessibility and stability of beta-carotene, *Food Funct.*, 2017, **8**(4), 1438–1451.
27 Y. Tian and N. C. Acevedo, Kinetic study on photostability of retinyl palmitate entrapped in policosanol oleogels, *Food Chem.*, 2018, **255**, 252–259.
28 F. R. Lupi, D. Gabriele, N. Baldino, L. Seta and B. de Cindio, A rheological characterisation of an olive oil/fatty alcohols organogel, *Food Res. Int.*, 2013, **51**, 510–517.
29 M. Scalzo, E. Santucci, F. Cerreto and M. Carafa, Model lipophilic formulations of retinyl palmitate: influence of conservative agents on light-induced degradation, *J. Pharm. Biomed. Anal.*, 2004, **34**(5), 921–931.
30 H. Y. Carr and E. M. Purcell, Effects of diffusion on free precession in nuclear magnetic resonance experiments, *Phys. Rev.*, 1954, **94**, 630–638.

31 S. Meiboom and D. Gill, Modified spin-echo method for measuring nuclear relaxation times, *Rev. Sci. Instrum.*, 1958, **29**, 668–691.
32 *AOCS official method cd 8b-90*, 2011.
33 P. A. Murphy, R. Engelhardt and S. E. Smith, Isomerization of retinyl palmitate in fortified skim milk under retail fluorescent lighting, *J. Agric. Food Chem.*, 1988, **36**(3), 592–595.
34 M. A. Rogers and A. G. Marangoni, Non-isothermal nucleation and crystallization of 12-hydroxystearic acid in vegetable oils, *Cryst. Growth Des.*, 2008, **8**(12), 4596–4601.
35 A. I. Blake and A. G. Marangoni, Structure and physical properties of plant wax crystal networks and their relationship to oil binding capacity, *J. Am. Oil Chem. Soc.*, 2014, **91**(6), 885–903.
36 E. Dibildox-Alvarado, J. N. Rodrigues, L. A. Gioielli, J. F. Toro-Vazquez and A. G. Marangoni, Effects of crystalline microstructure on oil migration in a semisolid fat matrix, *Cryst. Growth Des.*, 2004, **4**(4), 731–736.
37 T. Laredo, S. Barbut and A. G. Marangoni, Molecular interactions of polymeroleogelation, *Soft Matter*, 2011, **7**(6), 2734–2743.
38 A. Gravelle, M. Davidovich-Pinhas, A. Zetzl, S. Barbut and A. Marangoni, Influence of solvent quality on the mechanical strength of ethylcellulose oleogels, *Carbohydr. Polym.*, 2016, **135**, 169–179.
39 M. Pignitter, B. Dumhart, S. Gartner, F. Jirsa, G. Steiger, K. Kraemer and V. Somoza, Vitamin A is rapidly degraded in retinyl palmitate-fortified soybean oil stored under household conditions, *J. Agric. Food Chem.*, 2014, **62**(30), 7559–7566.
40 R. Steele, *Understanding and measuring the shelf-life of food*, Woodhead Publishing, 2004.